Magnetic phase diagram of the $La_{0.88}MnO_x$ ($2.82 \leq x \leq 2.96$) system

2003 J. Phys.: Condens. Matter 15 6005

(http://iopscience.iop.org/0953-8984/15/35/309)

INSTITUTE OF PHYSICS PUBLISHING JOURNAL OF PHYSICS: CONDENSED MATTER

J. Phys.: Condens. Matter **15** (2003) 6005–6015 PII: S0953-8984(03)63083-3

Magnetic phase diagram of the $La_{0.88}MnO_x$ ($2.82 \leqslant x \leqslant 2.96$) system

I O Troyanchuk[1,3], V A Khomchenko[1], A N Chobot[1] and H Szymczak[2]

[1] Institute of Solid State and Semiconductor Physics, National Academy of Sciences, P Brovka street 17, 220072 Minsk, Belarus

[2] Institute of Physics, Polish Academy of Sciences, Lotnikov Street 32/46, 02-668 Warsaw, Poland

E-mail: troyan@ifttp.bas-net.by

Received 1 May 2003
Published 22 August 2003
Online at stacks.iop.org/JPhysCM/15/6005

Abstract

The crystal structure and elastic and magnetic properties of the $La_{0.88}MnO_x$ ($2.82 \leqslant x \leqslant 2.96$) series as a function of oxygen content have been investigated. The crystal structure of the samples has been found to be orthorhombic at $x < 2.91$ and monoclinic at $x \geqslant 2.91$ depending on the oxygen concentration. Both crystal structure and elastic properties indicate the presence of static ($x < 2.87$) or dynamic ($x \geqslant 2.87$) Jahn–Teller distortions under the whole range of doping. The strong correlation between the type of orbital state and magnetic properties of the samples is revealed. It is shown that compounds with an antiferromagnetic component have features of orbital ordering while ferromagnetic samples are orbitally disordered. The magnetic phase diagram of the $La_{0.88}MnO_x$ ($2.82 \leqslant x \leqslant 2.96$) system is proposed on the basis of results obtained.

1. Introduction

Interest in the study of substituted lanthanum manganites has increased sharply as a result of the colossal magnetoresistance revealed in this class of compounds, reaching $10^5\%$ at $T \sim 100$ K [1, 2]. The nature of the interplay between the magnetic and electric properties of these materials is still a matter of discussion despite numerous investigations. Some models of exchange interactions have been proposed to explain a magnetic state evolution under hole doping as well as a metal–insulator transition at the Curie point. The most popular is a double-exchange theory assuming the antiferromagnet–ferromagnet transition occurs through a canted magnetic structure [3]. However, some facts evidence a mixed magnetic state might be realized in lanthanum manganites [4, 5], which is often interpreted in terms of electron and impurity

[3] Author to whom any correspondence should be addressed.

phase separation [6, 7]. Taking into account the orbital ordering effect Goodenough *et al* [8, 9] supposed that, together with double exchange, ferromagnetism in manganites is due to a specific character of superexchange interactions in Mn^{3+}–O–Mn^{3+} and Mn^{3+}–O–Mn^{4+} systems containing Jahn–Teller ions.

The parent $LaMnO_3$ compound is an A-type antiferromagnet [10] with $T_N = 140$ K and small ferromagnetic moment caused by Dzyaloshinskii's antisymmetric interaction [11]. In this compound, the transition to the ferromagnetic state takes place by La ion substitution for divalent alkaline earth ones or by oxidation of the stoichiometric sample, the oxygen nonstoichiometry being accommodated by the appearance of an equal number of cation vacancies in A- and B-sublattices of ABO_3 perovskite. The majority of publications on the present subject is devoted to these methods.

Another method of ferromagnetic ordering realization in lanthanum manganites proposed recently is connected with formation of La^{3+} cation deficiency [12]. Compounds show different properties at the same lanthanum deficiency [13–15]. So, the La-deficient sample study is of interest in dependence on oxygen content, similar to the $LaMnO_{3+\delta}$ system. As far as we know no detailed investigation of this problem has been carried out.

In the present paper we have found that the $La_{0.88}MnO_x$ system can be in different orbital and magnetic states depending on the oxygen content, and orbital order–disorder and antiferromagnet–ferromagnet transitions occur at the same time. It is assumed that these transitions take place by means of two-phase state realization.

2. Experimental details

Standard ceramic technology has been used to prepare polycrystal $La_{0.88}MnO_x$ samples. After prefiring a La_2O_3 and Mn_2O_3 mixture at 950 °C for 2 h, the obtained product was ground, pressed into pellets, annealed at $T = 1300$ °C in air for 6 h, and then cooled at a rate of 50 °C h^{-1}. The oxygen content of the resulting material has been determined using thermogravimetric analysis (TGA) by decomposition into simple oxides La_2O_3 and MnO in a reducing H_2/N_2 flow. The true formula of the obtained compound was $La_{0.88}MnO_{2.96}$. The reduction of the samples was carried out in evacuated quartz ampoules at $T = 1050$ °C for a long time (24 h) to avoid chemical heterogeneity. Metallic tantalum was used as reducing agent.

The unit cell parameters as well as the phase purity of the samples were checked by x-ray analysis using a DRON-3 diffractometer with Cr Kα radiation. Magnetization measurements were made with an OI-3001 commercial vibrating-sample magnetometer. Elastic properties were investigated by the resonance method in a sound frequency range using samples in the form of a rod with length of 60 mm and diameter of 6 mm. Neutron diffraction measurements for the $La_{0.88}MnO_{2.87}$ sample were performed in the Berlin Neutron Scattering Centre using the E9 neutron powder diffractometer (FIREPOD) with a neutron wavelength of $\lambda = 1.7974$ Å and scanning step $\Delta\Theta \sim 0.002°$. Both x-ray and neutron diffraction data were analysed with the Rietveld method using the FullProf program [16].

3. Results

In the process of this work we have managed to obtain samples of the $La_{0.88}MnO_x$ system in the oxygen concentration range $2.82 \leqslant x \leqslant 2.96$. This range corresponds to manganese average valence from 3 to 3.28. Reduction below the value of 2.82 leads to decomposition of the samples into La_2O_3 and MnO oxides. This means that the structure of the $La_{0.88}MnO_x$ perovskite cannot accommodate an appreciable number of Mn^{2+} ions.

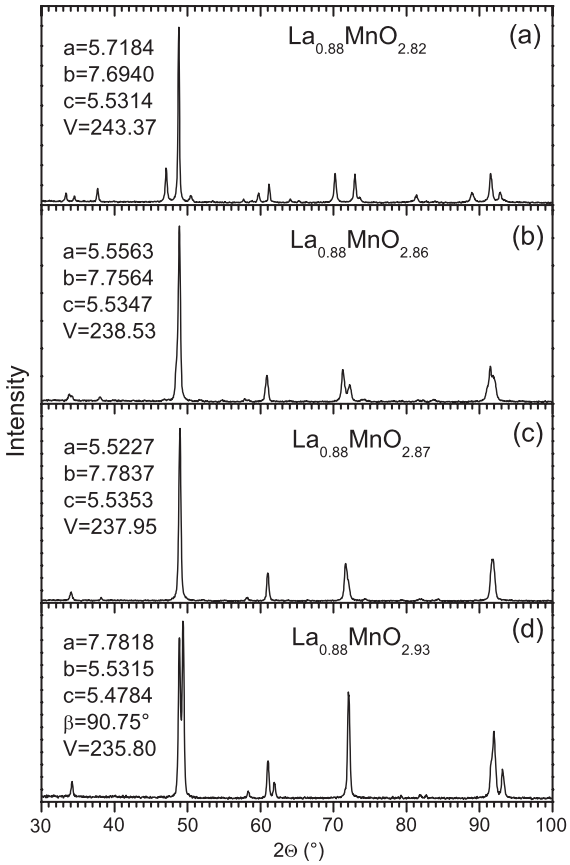

Figure 1. Room-temperature x-ray powder diffraction patterns of $La_{0.88}MnO_x$ samples with different oxygen content. Unit cell values (in Å) are presented.

According to x-ray diffraction data the $La_{0.88}MnO_x$ ($2.82 \leqslant x \leqslant 2.86$) samples are characterized by the so-called O′-orthorhombic type of unit cell distortion ($b/\sqrt{2} < c < a$), space group $Pnma$ (figures 1(a), (b)). Unit cell values of the most reduced $La_{0.88}MnO_{2.82}$ compound have been found to be very close to those for the $LaMnO_3$ stoichiometric composition [17–19]. Unit cell volume decreases as oxygen content increases, and the transition to the O-orthorhombic crystal structure ($b/\sqrt{2} \approx a < c$) occurs starting from the $x = 2.87$ compound (figure 1(c)). It is worth noting that, according to the consideration of Goodenough *et al* [8], O′-orthorhombic distortions in manganites are due to an orbital ordering while O-orthorhombic structure corresponds to the orbitally disordered state. It is obvious that the transition to the orbitally disordered state as oxygen concentration increases is the result of the appearance of a sufficient number of Mn^{4+} ions which remove the Jahn–Teller cooperative static effect. The $La_{0.88}MnO_x$ ($2.91 \leqslant x \leqslant 2.96$) compounds are accounted for in monoclinic syngony (space group $I2/a$) (figure 1(d)). The transition from orthorhombic to monoclinic symmetry observed in La-deficient manganites with increase of the oxygen content is corroborated by electron and x-ray diffraction measurements [15].

The results of study of the Young's modulus temperature dependence for samples with different oxygen contents (the square of the resonance frequency is proportional to Young's modulus) are presented in figure 2. The most reduced, $La_{0.88}MnO_{2.82}$, sample shows a well

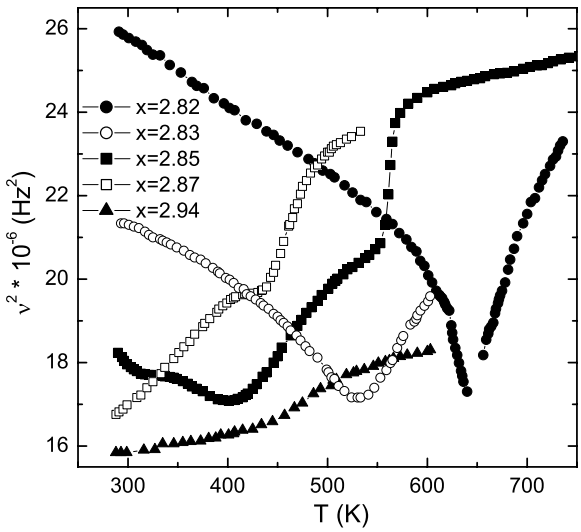

Figure 2. The square of the resonance frequency (proportional to Young's modulus) as a function of temperature for $La_{0.88}MnO_x$ ($2.82 \leqslant x \leqslant 2.94$) samples.

pronounced crystal structure phase transition around 650 K. A temperature hysteresis of about 12 K and strong attenuation are observed in the vicinity of 650 K. It is noteworthy that a similar transition observed for the $LaMnO_3$ stoichiometric compound at a close temperature [20] is associated with a removal of orbital ordering. As oxygen content increases the temperature of the phase transition reduces gradually and the transition becomes broader. The temperature of the orbital order–disorder phase transition for $x = 2.83$ and 2.85 compounds decreases down to 530 and 400 K, respectively. Moreover, a sharp increase of the Young's modulus value is observed for the $La_{0.88}MnO_{2.85}$ sample around 560 K. The temperature hysteresis of about 20 K indicates a first-order crystal structure transition. For the $x = 2.86$ compound, the temperature dependence of the Young's modulus exhibits a broad minimum associated with the transition to the orbitally disordered state slightly above room temperature. The temperature of the second anomaly decreases down to 500 K. In contrast to $2.82 \leqslant x \leqslant 2.86$ samples, there are no features of cooperative orbital ordering for the $La_{0.88}MnO_{2.87}$ compound, but a significant increase of the Young's modulus value is also observed above 440 K. The monoclinic compounds do not show sharp changes in the behaviour of Young's modulus and exhibit a gradual increase of resonance frequency in the whole accessible temperature range. It is worth noting that usually a resonance frequency decreases with temperature. An anomalous increase of Young's modulus reflects an instability of crystal structure which can be attributed to the dynamic Jahn–Teller effect.

In order to reveal the origin of the sharp increase of the Young's modulus value which was observed for both orbitally ordered and orbitally disordered $2.85 \leqslant x \leqslant 2.87$ compounds we performed a neutron diffraction study of the $La_{0.88}MnO_{2.87}$ sample. The diffraction patterns were obtained below and above the temperature of the phase transition. The structural data calculated using the Rietveld refinement are presented in table 1. According to the obtained results the crystal structure of $La_{0.88}MnO_{2.87}$ sample at $T = 300$ K is characterized by an orthorhombic type of unit cell distortion. The space group *Pnma* was used for the refinement. At 500 K, Bragg reflections which are forbidden by the space group *Pnma* were observed. The crystal structure at 500 K was found to be monoclinic (space group $I2/a$). The observed and

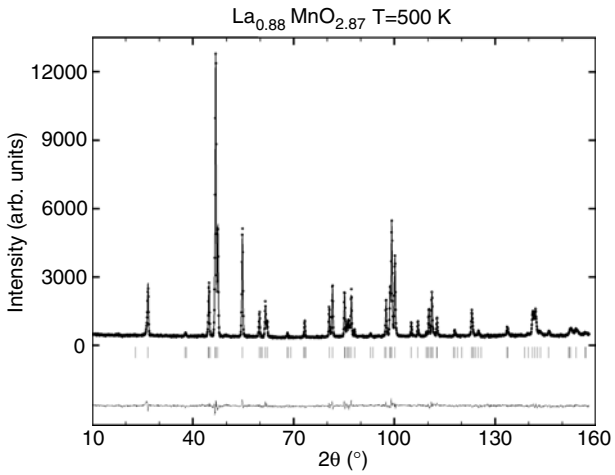

Figure 3. Observed and calculated powder diffraction patterns of $La_{0.88}MnO_{2.87}$ at 500 K.

Table 1. Structural data of the $La_{0.88}MnO_{2.87}$ sample at 300 and 500 K.

T (K)	Cell (Å)	Atoms	x	y	z	R-factors (%)
	$a = 5.5227(3)$	La 4c	0.0209(3)	0.2500	0.9955(3)	$R_p = 4.54$
300	$b = 7.7836(8)$	Mn 4b	0.0000	0.0000	0.5000	$R_{wp} = 5.8$
Pnma	$c = 5.5353(3)$	O1 4c	0.4944(7)	0.2500	0.0664(2)	$R_B = 4.79$
	$\alpha = \beta = \gamma = 90°$	O2 8d	0.2215(8)	0.5335(1)	0.2290(9)	$\chi^2 = 1.99$
	$a = 7.8220(8)$	La 4e	0.2500	0.5023(5)	0.0000	$R_p = 4.75$
500	$b = 5.5575(2)$	Mn 4a	0.0000	0.0000	0.0000	$R_{wp} = 6.1$
*I*2/*a*	$c = 5.5043(4)$	O1 4e	0.2500	0.0597(7)	0.0000	$R_B = 5.42$
	$\alpha = \gamma = 90°; \beta = 90.78(2)°$	O2 8f	−0.0214(6)	0.2160(9)	0.2781(1)	$\chi^2 = 2.21$

calculated diffraction patterns obtained for the $La_{0.88}MnO_{2.87}$ sample at 500 K are shown in figure 3. Thus, neutron diffraction data indicate that anomalous behaviour of the Young's modulus temperature dependence observed for the $x = 2.87$ compound above 440 K is associated with the transition from the orthorhombic to monoclinic type of unit cell distortion.

The study of magnetic properties has revealed a correlation between the types of magnetic and orbital state. The results of magnetization measurements versus field for the $La_{0.88}MnO_x$ system at $T = 5$ K are presented in figures 4 and 5. The $La_{0.88}MnO_{2.82}$ sample with the lowest oxygen content has a very small spontaneous magnetic moment (about 0.09 μ_B per manganese ion) and very large coercive field (−15 kOe). Magnetization versus temperature for this sample is shown in figure 6. A sharp transition into the paramagnetic state is observed at a temperature of 140 K. The external magnetic field practically does not shift the temperature of phase transition. Increase of oxygen content in the concentration range corresponding to O′-orthorhombically distorted compositions results in Néel point lowering (figures 7(a)–(c)) and spontaneous magnetization increase (figure 4). For example, the spontaneous magnetization of the $x = 2.84$ compound is 0.5 μ_B/Mn, the coercive field is 4.2 kOe and the temperature of magnetic ordering is 125 K (figure 7(b)). The transition into the paramagnetic state remains well pronounced. External magnetic field weakly affects the temperature of transition into the paramagnetic state, similar to the case of the $x = 2.82$ composition. The tendency of

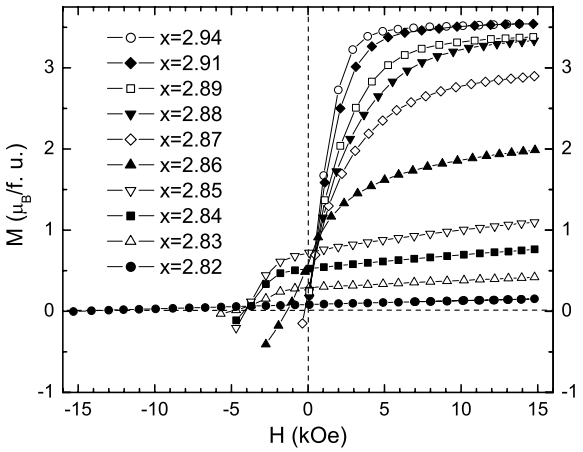

Figure 4. Magnetization versus field for $La_{0.88}MnO_x$ ($2.82 \leqslant x \leqslant 2.94$) compounds at $T = 5$ K.

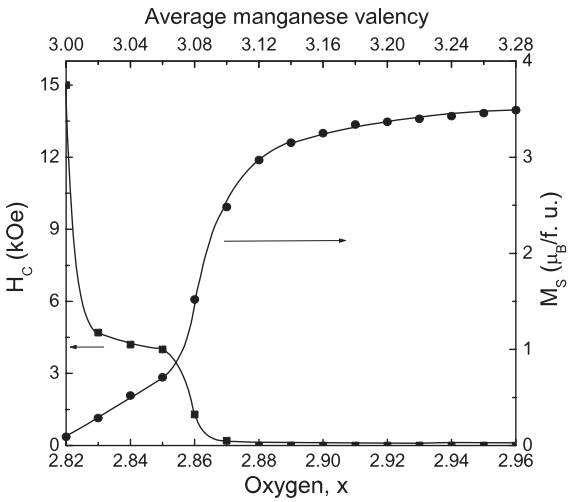

Figure 5. Magnetic moments per Mn ion at $T = 5$ K and coercive field for $La_{0.88}MnO_x$ ($2.82 \leqslant x \leqslant 2.96$) compounds depending on x.

the magnetic ordering temperature to decrease remains up to the $La_{0.88}MnO_{2.85}$ compound (figure 7(c)).

The magnetic state changes sharply with the further increase of oxygen concentration in the range of the orthorhombically distorted samples. Starting from $x = 2.86$ the temperature of magnetic ordering increases from 150 K ($x = 2.86$) to 202 K ($x = 2.90$), and a considerable rise of the spontaneous magnetization up to 3.25 μ_B/Mn for $x = 2.90$ is observed. Besides, the magnetic anisotropy and coercive field decrease significantly (figures 5 and 7(d)–(g)).

The maximal spontaneous magnetization value (up to 3.5 μ_B/Mn), close to that expected for a collinear ferromagnet, has been obtained for monoclinic distorted compounds (figure 5). FC and ZFC curve behaviour indicates that the monoclinic samples undergo the paramagnet–ferromagnet transition at temperatures from 212 K for $La_{0.88}MnO_{2.91}$ to 255 K for $La_{0.88}MnO_{2.96}$ (figures 7(h) and (i)). In contrast to O′-orthorhombic samples an external field

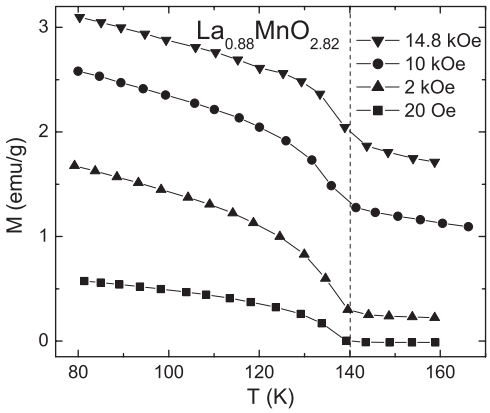

Figure 6. Temperature dependence of magnetization for the $La_{0.88}MnO_{2.82}$ sample at different magnetic fields.

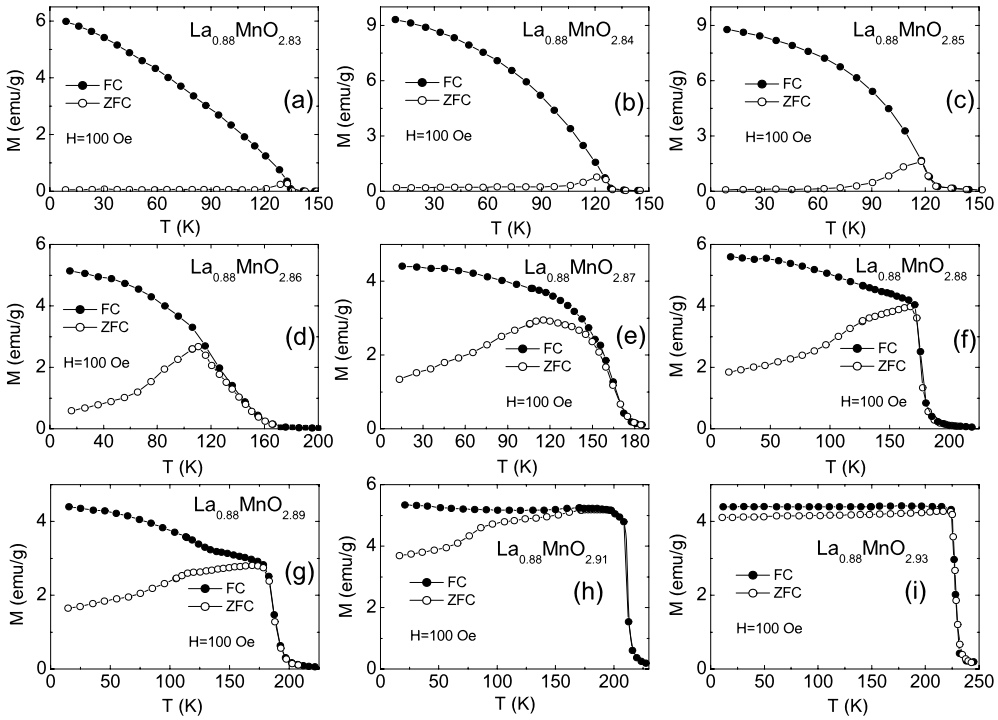

Figure 7. FC and ZFC magnetization of the $La_{0.88}MnO_x$ compounds, measured at 100 Oe.

shifts the transition rather far to higher temperatures. Note that T_C values for the $La_{0.88}MnO_x$ compound are higher than observed for $LaMnO_{3+\delta}$ samples corresponding to the same limits of Mn^{4+}/Mn^{3+} ratio [21].

4. Discussion

The stoichiometric $LaMnO_3$ is known to be an orbitally ordered antiferromagnet with the Néel temperature of 140 K [22]. Cooperative ordering of d_{z^2} orbitals observed for this compound

is removed around 700 K at the first-order phase transition [20]. The properties of the most strongly reduced sample $La_{0.88}MnO_{2.82}$ are similar to the properties of the stoichiometric $LaMnO_3$. The $x = 2.82$ compound has the same $T_N = 140$ K (figure 6), and exhibits the features of cooperative orbital ordering (figure 2). The existence of orbital ordering responsible for the A-type antiferromagnetic structure in the $La_{0.88}MnO_{2.82}$ is corroborated by neutron diffraction measurements [13]. On the other hand, the reduced $La_{0.7}Ca_{0.3}MnO_{2.85}$, which does not contain Mn^{4+} ions either, is a spin glass with the temperature of magnetic moments freezing around 40 K; it does not show features of cooperative orbital ordering [23]. This results from an oxygen vacancy appearance changing the character of exchange interactions between manganese ions and removing the orbital ordering [23]. Really, d_{z^2} orbitals of Mn^{3+} ions in pentahedron coordination are directed as a rule to oxygen vacancies, which does not agree with cooperative orbital ordering taking into account the statistical distribution of oxygen vacancies. Therefore one can believe that oxygen vacancies do not appear in $La_{0.88}MnO_x$.

It is well known that the oxygen nonstoichiometry in $LaMnO_{3+\delta}$ is accommodated through the cation vacancies because the perovskite structure cannot accept excess oxygen in an interstitial site [12]. Accordingly, the composition of $LaMnO_{3+\delta}$ is expressed as $La_{1-\varepsilon}Mn_{1-\varepsilon}O_3$, where $\varepsilon = \delta/(3 + \delta)$. Structural defects in La-deficient manganites were studied by neutron diffraction coupled with sample density measurements [24, 25]. It was shown that the defect structure of the sample of nominal composition $La_{0.91}MnO_{2.961}$ is realized as $[La_{0.922}Mn_{0.013}]MnO_3$. The resulting distribution model, $[La_{6(1-x)}Mn_{3(1+x)-V}]_{1/[3(1-x)+V]}MnO_3$ (where x is the nominal La deficiency, and V is the average oxidation state of Mn ions), is characterized by conservation of the oxygen skeleton. The excess of Mn ions is located on the La sites. In such a model, the nominal sample $La_{0.88}MnO_{2.82}$ does not contain the vacancies in the A-sublattice of the ABO_3 perovskite and has a cationic composition which is very close to that for the stoichiometric $LaMnO_3$. Consequently, one could expect that the properties of these two compounds will be similar. Indeed, both compositions have very close unit cell parameters (figure 1), the same spontaneous magnetization value (figure 4) and very close temperatures of magnetic ordering (figure 6) and orbital ordering (figure 2). Moreover, the proposed model of structural defects is able to explain the increase of T_C for the $La_{0.88}MnO_x$ compounds in comparison with $LaMnO_{3+\delta}$ samples as a result of conservation of MnO_6 octahedrons and the absence of Mn vacancies in the B-sublattice. On the other hand, according to both [25] and our neutron diffraction data, the best fitting is observed in the model of the nominal chemical composition. The determination of structural defects in La-deficient manganites is beyond the framework of this paper. Below we refer to the nominal compositions. The mechanism of nonstoichiometry realization in the $La_{0.88}MnO_x$ system will be revealed in the further research.

As oxygen content increases up to $x = 2.85$ magnetic and orbital ordering temperatures decrease whereas spontaneous magnetization increases (figures 2, 5 and 7(a)–(c)). Such a behaviour inherent in $La_{1-x}A_xMnO_3$ (A–Ca, Sr, Ba; $x < 0.05$) manganites could be explained with either formation of canted magnetic structure (double-exchange model) [3], or appearance of ferromagnetic clusters with the higher charge carrier concentration (electronic phase separation) [6]. The double-exchange mechanism was proposed by Zener [26] in order to explain the appearance of the metallic ferromagnetic phase in manganites. Zener proceeded from the assumption that the spin of the delocalized electron should be parallel to the spin of the localized ion owing to a strong exchange interaction between the charge carrier and the localized spin. If spins of two ions Mn^{3+} and Mn^{4+} are parallel the electron would move between them, reducing the total energy of the system. The theory of double exchange for the case of a crystal was developed by De Gennes [3], who predicted that transition from an antiferromagnetic state to a ferromagnetic one should occur by means of canted

magnetic structure appearance. Against the latter assertion there are a number of theoretical objections [6, 7]. The fact is that non-homogeneous collinear structures can be more favourable in comparison with a homogeneous canted state; in other words, the system tends to a two-phase state. Here, a minimum of energy is achieved due to accumulation of charge carriers in ferromagnetic regions. The difficulties in determination of priority of the present models are conditioned by the fact that two-phase collinear structure can exhibit itself in experiments in the same way as the homogeneous canted phase. For example, data of neutron diffraction investigations are interpreted both within the framework of a canted model [27] and in the supposition of realization of a two-phase state [10]. The results of NMR experiments may be better understood on the assumption of a phase separation scenario [28]. On the other hand, separation into regions with different concentrations of electrons leads to a strong Coulomb repulsion, therefore these phases could coexist only in the form of the smallest 'drops' [29]; however, experimental data reveal a presence of ferromagnetic clusters with a size up to 100–1000 Å [30–32]. An alternative mechanism for the antiferromagnet–ferromagnet transition was offered by Goodenough (for example, see [8]). According to the rules for 180° superexchange, if the electronic configuration correlates with vibrational modes, Mn^{3+}–O^{2-}–Mn^{3+} interactions are antiferromagnetic in the case of the static Jahn–Teller effect and ferromagnetic when the Jahn–Teller effect is dynamic. Thus, antiferromagnetic–ferromagnetic phase transition can occur through a mixed state of phases with different orbital dynamics.

A number of observed experimental data provide evidence in favour of the magnetic phase separation model and confirm a key role of the orbital ordering effect for the formation of the antiferromagnet–ferromagnet transition in low-doped manganites. Firstly, magnetic properties of the investigated compounds correlate with the type of orbital state. Compounds with a significant antiferromagnetic component reveal the features of cooperative orbital ordering, while ferromagnetic samples are orbitally disordered. The anomalous behaviour of their elastic properties can be explained by the dynamic Jahn–Teller effect. Secondly, a decrease of the Néel point (up to the $x = 2.85$ compound) followed by a sharp decrease of the coercive field and magnetic anisotropy as well as an increase of spontaneous magnetization (figure 5) are easily explained in the framework of the two-phase percolation model. Moreover, the broadening of the transition into the paramagnetic state which is observed for the samples in the intermediate range of doping (figures 7(d) and (e)) supports the two-phase model too. The hypothetical magnetic phase diagram of the $La_{0.88}MnO_x$ ($2.82 \leqslant x \leqslant 2.96$) system is presented in figure 8. We believe that increase of oxygen concentration above $x = 2.82$ leads to the appearance of holes in 3d states of Mn ions (i.e. Mn^{4+} ion appearance). Orbital ordering is removed near Mn^{4+} ions, and exchange interactions between Mn ions become ferromagnetic. The number of orbitally disordered ferromagnetic clusters increases with increase of oxygen content. This leads to lowering of the Néel point (figure 8) and increase of spontaneous magnetization (figure 5). Simultaneously, the temperature of orbital ordering removal decreases (figure 2). The significant decrease of the coercive field and increase of the spontaneous magnetization observed starting from $x = 2.86$ (figure 5) denote the percolation of ferromagnetic clusters. At the same time x-ray diffraction data as well as the Young's modulus temperature dependence presume a conservation of the orbitally ordered phase up to the $x = 2.87$ compound. In other words, the two-phase state is realized in the range $2.85 < x < 2.87$ (figure 8). The first phase is orbitally disordered ferromagnetic while the second one is orbitally ordered antiferromagnetic. With further increase of oxygen concentration the size of the antiferromagnetic phase gradually decreases. The low-temperature anomaly observed in the temperature dependence of the ZFC magnetization for $2.87 \leqslant x \leqslant 2.91$ samples (figures 7(f)–(h)) presumes a conservation of antiferromagnetic clusters up to the concentration range of monoclinic distorted compounds (figure 8). The value of spontaneous magnetization of the monoclinic samples $x \geqslant 2.92$

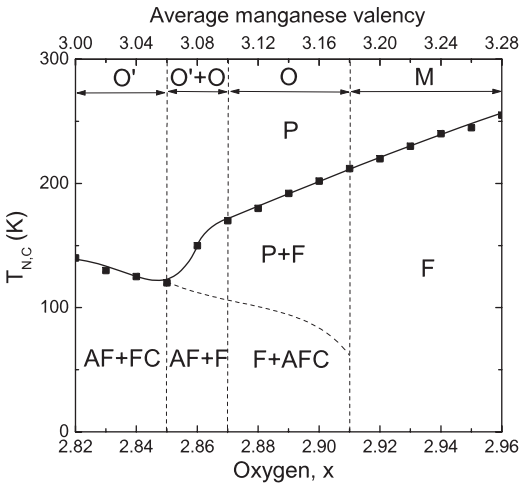

Figure 8. Magnetic phase diagram of the $La_{0.88}MnO_x$ ($2.82 \leqslant x \leqslant 2.96$) system. O′, orbitally ordered orthorhombic crystal structure; O, orbitally disordered orthorhombic crystal structure; M, monoclinic crystal structure; P, AF, F, paramagnetic, antiferromagnetic, and ferromagnetic states, respectively; FC, AFC, ferromagnetic and antiferromagnetic clusters.

presumes the collinear ferromagnetic state (figure 5). The key influence of the type of orbital state on the magnetic and transport properties of low-doped manganites as well as possibility of co-existence of orbitally ordered and orbitally disordered phases are confirmed by x-ray and neutron diffraction data [33, 34].

5. Conclusion

A detailed study of crystal structure and elastic and magnetic properties of samples of the $La_{0.88}MnO_x$ ($2.82 \leqslant x \leqslant 2.96$) system was carried out. The most reduced $La_{0.88}MnO_{2.82}$ sample containing only Mn^{3+} ions was shown to be an antiferromagnet with $T_N = 140$ K. It was revealed that its properties are very similar to those for the $LaMnO_3$ stoichiometric compound. The crystal structure of the investigated compounds was found to undergo a number of concentration transitions: from orbitally ordered orthorhombic to orbitally disordered orthorhombic, and then to monoclinic. It was shown that the magnetic state of the samples of the $La_{0.88}MnO_x$ system strongly correlates with the type of orbital ordering. The compounds with an antiferromagnetic component exhibit the features of cooperative orbital ordering, while pure ferromagnetic samples, with T_C up to 255 K for $x = 2.96$, are orbitally disordered. The antiferromagnet–ferromagnet phase transition was described in the framework of an intermediate two-phase state realization. From the analysis of the experimental results the magnetic phase diagram was constructed.

Acknowledgments

The work was partly supported by the Belarus Fund for Basic Research (project F01-039), the Polish State Committee for Scientific Research (grant 5 P03B 016 20) and Deutsche Forschungsgemeinschaft (Germany).

References

[1] McCormack M *et al* 1994 *Appl. Phys. Lett.* **64** 3045
[2] Jin S *et al* 1994 *Science* **264** 413
[3] De Gennes P G 1960 *Phys. Rev.* **118** 141
[4] Allodi G *et al* 1997 *Phys. Rev.* B **56** 6036
[5] Troyanchuk I O 1992 *Sov. Phys.—JETP* **75** 132
[6] Nagaev E L 2001 *Phys. Rep.* **346** 387
[7] Dagotto E, Hotta T and Moreo A 2001 *Phys. Rep.* **344** 1
[8] Goodenough J B *et al* 1961 *Phys. Rev.* **124** 373
[9] Zhou J-S, Yin H Q and Goodenough J B 2001 *Phys. Rev.* B **63** 184423
[10] Wollan E O and Koehler W C 1955 *Phys. Rev.* **100** 545
[11] Dzyaloshinskii I E 1958 *J. Solid State Chem.* **4** 241
[12] Van Roosmalen J A M *et al* 1994 *J. Solid State Chem.* **110** 100
[13] Hauback B C, Fjellag H and Sakai N 1996 *J. Solid State Chem.* **124** 43
[14] Topfer J and Goodenough J B 1997 *Chem. Mater.* **9** 1467
[15] Maignan A *et al* 1997 *Solid State Commun.* **101** 277
[16] Rodriguez-Carvajal J 1993 *Physica* B **12** 55
[17] Norby P 1995 *J. Solid State Chem.* **119** 191
[18] Huang Q 1997 *Phys. Rev.* B **55** 14987
[19] Rodriguez-Carvajal J *et al* 1998 *Phys. Rev.* B **57** 3189
[20] Kasper N V and Troyanchuk I O 1996 *J. Phys. Chem. Solids* **57** 1601
[21] Topfer J and Goodenough J B 1997 *J. Solid State Chem.* **130** 117
[22] Matsumoto G 1970 *J. Phys. Soc. Japan* **29** 606
[23] Troyanchuk I O *et al* 2001 *JETP* **93** 161
[24] Horyn R, Sikora A and Bukowska E 2003 *J. Alloys Compounds* **353** 153
[25] Wolcyrz M *et al* 2003 *J. Alloys Compounds* **353** 170
[26] Zener C 1951 *Phys. Rev.* **82** 403
[27] Jirak Z, Vratislav S and Zajicek J 1979 *Phys. Status Solidi* a **52** K39
[28] De Renzi R *et al* 2000 *Physica* B **289/290** 85
[29] Gor'kov L P and Sokol A V 1987 *JETP Lett.* **46** 333
[30] Uehara M *et al* 1999 *Nature* **399** 560
[31] Balagurov A M *et al* 2001 *Eur. Phys. J.* B **19** 215
[32] Mori S, Chen C H and Cheong S-W 1998 *Nature* **392** 473
[33] Van Aken B B *et al* 2003 *Phys. Rev. Lett.* **90** 066403
[34] Dabrowski B *et al* 1999 *J. Solid State Chem.* **146** 448